In vivo measurements of penetration depth, oxygenation, and drug concentration using broadband absorption spectroscopy in human tissues before and after photodynamic therapy

Hsing-Wen Wang*[a], Tim C. Zhu[b], Michael Solonenko[a], Stephen M. Hahn[b], James Metz[b], Andreea Dimofte[b], Jermy Mile[b], and Arjun G. Yodh[a*]
[a]Department of Physics and Astronomy, University of Pennsylvania, 209 S 33rd St., Philadelphia, PA USA 19104-6396
[b]Department of Radiation Oncology, University of Pennsylvania, 3620 Hamilton Walk, Philadelphia, PA 19104-6072

ABSTRACT

Photodynamic therapy (PDT) employs a combination of photosensitizing chemical, light, and oxygen Knowledge of tissue optical properties, including absorption (μ_a) and reduce scattering coefficients (μ_s'), makes possible to derive blood oxygen saturation, light penetration depth, and drug concentration, which are important to ensure PDT treatment efficacy at the specific wavelengths. We have developed an absorption spectroscopy system to measure μ_a and μ_s' in the spectral range 600-800nm using a contact linear probe with a source fiber and multiple source-detector separation distances less than 1 cm. The μ_a and μ_s' were recovered based on diffusion approximations of the photon transport equation. We measured tissue optical properties among various organs of patients with intraperitoneal malignancies for an on-going Phase II PDT protocol. The results from 12 patients showed various effective penetration depth from site to site and from organ to organ. The percentage oxygen saturation ($\%S_tO_2$) are similar before and after PDT. Before PDT, μ_{eff} (mean (standard deviation) (number of patients)) in cm^{-1} at 630nm are 2.4 (0.2) (12) in small bowel, 2.2(0.4) (9) in large bowel, 4.2(2.7) (7) in tumor, 3.3 (0.3) (10) in peritoneum, 2.7 (0.3) (11) in skin, and 10.1 (0.6) (10) in liver. $\%S_tO_2$ is 60-80% for most organs but 30-40% for tumor.

Keywords: Photodynamic therapy, diffuse photon density wave spectroscopy, broadband absorption spectroscopy.

1. INTRODUCTION

Photodynamic therapy (PDT) is currently being evaluated as an adjuvant to surgery to treat solid tumors and surface malignancies by administrate photosensitizer around tumor cells. In the presence of oxygen, the irradiation of photosensitizer at appropriate wavelength initiates a cascade of chemical reactions, often involving highly reactive oxygen intermediates that can produce selective tumor regression and destruction. Therefore, the efficacy of PDT depends on sufficient concentrations of photons, photosensitizer, and oxygen in the tumor tissue. The relationship between the distribution and concentration of the light dose and photosensitizer distribution and the supply of oxygen during PDT is tissue dependent and dynamic.

Clinical PDT dosimetry is limited. Typically a total light dose is measured at a 5mmX5mm tissue area, but no account is explicitly taken for tissue optical properties at specific wavelength (λ) including absorption ($\mu_a(\lambda)$) and reduce scattering coefficients ($\mu_s'(\lambda)$), or drug concentration. These quantities can be derived from optical absorption and emission measurements. The absorption coefficient μ_a permits the extraction of

* hwwang@dept.physics.upenn.edu; phone 1 215 573-6404; fax 1 215 898-0090

the percentage oxygen saturation. The μ_a and μ_s' can be used to determine the effective attenuation coefficient (μ_{eff}) and the light penetration depth ($\delta = 1/\mu_{eff}$) for uniform light illumination.

We have developed a broadband absorption spectroscopy system to measure μ_a and μ_s' in a wide spectral range (600-800nm) before and after PDT treatment among various organs for an on-going Phase II PDT protocol for patients with intraperitoneal malignancies. The probe consists of a fiber-optic-coupled light source and multiple detector fibers at different source-detector separation distances from 0.6 to 10.0mm to collect diffuse reflected light. The μ_a and μ_s' were recovered based on a diffusion approximation of the photon transport equation with restriction that μ_s' decreased as wavelength increased and has form $A\lambda^{-B}$. The system and analysis method were validated in measurements of tissue-like homogeneous Intralipid phantoms.

We have analyzed optical properties of various organs before and after PDT from 12 patients. Further data collection for more patients is undergoing to achieve statistically satisfactory sample size. The results, combined with current clinical PDT dosimetry, may provide important feedback to clinicians to improve PDT treatment.

2. METHODOLOGY

2.1 Instrument

We have built a broadband absorption spectrometer to simultaneously measure the wavelength-dependent reflectance of tissue at many source-detector separations. The schematic diagram of the system is shown in Figure 1. The system consists of four major parts: the light source, the fiber-optics probe head, the dispersion system (monochromator), and the CCD camera.

Light from a 250 W quartz tungsten halogen lamp (Cuda Fiberoptics) is coupled to the tissue surface through an optical fiber, the source fiber. The light is transmitted into the tissue and detected in the reflectance mode from the tissue surface by multiple detection fibers that were arranged in a line with various source-detector separation distances. The diffuse light reflected back from the tissue surface was collected by detector fibers and coupled back to the monochromator entrance slit.

At the entrance slit, the ends of the detector fibers are arranged in a vertical line with equal space and well positioned relative to the monochromator (300 g mm^{-1}, f/#=4, Acton Research, Acton, MA) such that the image of the fiber tips is focus on the liquid nitrogen cooled CCD camera sensor (Princeton Instruments). The grating disperses the light so that the image plan of monochromator output contains vertically spaced bright lines corresponding to the spectra, $R_{tissue}(\rho, \lambda)$ of detection fibers. The signal of each spectrum was binned across each detector line (27-35 vertical pixels). Between two detector lines, 2-5 vertical pixels were binned to account for the background light signals scattered inside the monochromator, $S_{tissue}(\rho, \lambda)$.

The nitrogen-cooled CCD camera has special pixel coating to efficiently collect light from 300 to 1000 nm. The pixel size is 24 μm and there are 330 (vertical) X 1100 (horizontal) pixels spreading over an area of 8 mm X 26 mm. The pixel noise is < 1 electron per second at 173 K, and the CCD has a quantum efficiency of 35% at 700nm. The spectral resolution is about 0.5nm/pixel for the grating with 300 groves/mm. The typical integration time for one measurement is 100 ms.

We have used two fiber-optics probe head to collect clinical IP-PDT data in the past two and half years. One probe consists of one source fiber and 6 detection fibers with 600 μm core diameter and source-detector separation distance ρ from 1.3 to 7.8 mm. These detection fibers were arranged equally spaced from each other. Another probe consists of one source fiber and 10 detection fibers with 400 μm core diameter and source-detector separation distance distances from 0.6 to 10 mm.

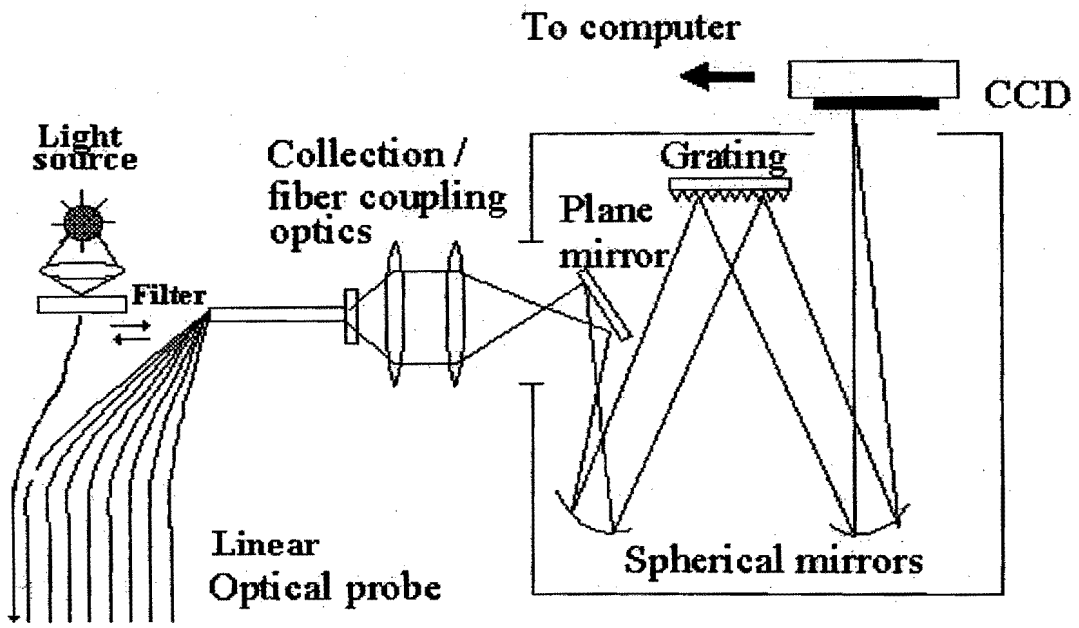

Figure 1: Schematic diagram of a broadband reflectance spectrometer including light source, fiber optical probe head, monochromator, and CCD camera.

2.2 Calibration and Data Analysis

The signal directly collected from tissue surface $R_{tissue}(\rho, \lambda)$ need to be corrected for the optical throughput of the detection system including detector fiber transmittance across the entire spectra region. We took an additional measurement $R_{sphere}(\rho, \lambda)$ immediately before or after each experiment from a 6-inch diameter integrating sphere (LabSphere, Inc.). A single optical fiber, coupling light from the same light source used in tissue, illuminated the integrating sphere through a 0.5-inch opening. The fiber-optics probe head was placed at another opening of the integrating sphere to collect a calibration signal $R_{sphere}(\rho, \lambda)$. Similar to tissue measurement, $S_{sphere}(\rho, \lambda)$ was obtained to account for the background signal. The effective measured reflectance $R_{measure}(\rho, \lambda)$ was then calculated as equation (1). $B_{tissue}(\rho, \lambda)$ and $B_{sphere}(\rho, \lambda)$ are the dark spectra collected with the light source off.

$$R_{measure}(\rho,\lambda) = \frac{R_{tissue}(\rho,\lambda) - S_{tissue}(\rho,\lambda) - B_{tissue}(\rho,\lambda)}{R_{sphere}(\rho,\lambda) - S_{sphere}(\rho,\lambda) - B_{sphere}(\rho,\lambda)} \quad (1)$$

Light travel inside the tissue can be described using the equation of radiative transfer (i.e. the transport equation). The transport equation is essential a conservation equation for the light radiance L(r,s) (unit: power per unit-length-squared per unit angle) at position r, traveling in direction s. The tissue properties that affect light transport are the absorption coefficient μ_a, the reduced scattering coefficient and μ_s' that has taken account for the probability of a scattering event for a photon traveling in the direction s into the direction s'.

In our measurement scheme that both source and detector fibers are on the same surface and separated by distance ρ along that surface, the reflectivity $R(\rho, \mu_a(\lambda), \mu_s'(\lambda))$ is modeled as a semi-infinite medium if the

As an example, Figure 2 shows the extracted reduced scattering, absorption, effective attenuation coefficients ($\mu_{eff} \approx \sqrt{3\mu_s'\mu_a}$), and penetration depth of small bowels as the function of the wavelength in the spectral range of 600-800 nm from all patients. The μ_s', μ_a, μ_{eff}, and penetration depth vary from 5 to 17, 0.07-0.55, 1.4-4.7 cm^{-1} and 2-7 mm at the treatment wavelength 630nm, respectively. The results before and after PDT are similar such that we only show the average results of optical properties of all organs before PDT in Figure 3. The numerical values of the μ_s', μ_a, μ_{eff}, and penetration depth at 630nm before and after PDT are listed in Table 2.

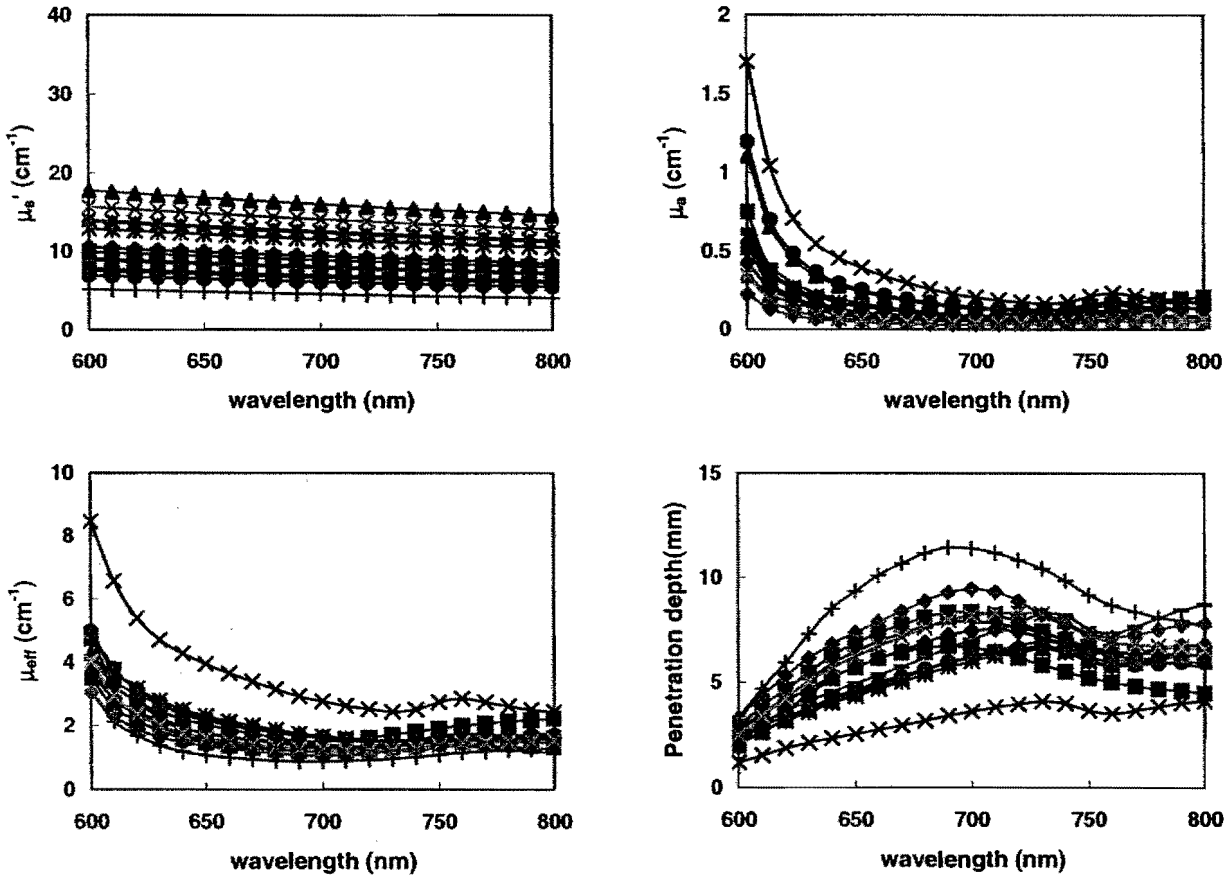

Figure 2. The optical properties of the small bowel, before PDT, from 12 patients in the spectral range of 600-800nm.

The μ_s' of tumor is similar to that of small bowel and large bowel. Peritoneum, skin, and liver tend to have higher μ_s' and variation (higher standard deviation). The penetration depth is calculated as $1/\mu_{eff}$ and has value 4.5-6mm at 630nm for small bowel and large bowel. Tumors tend to have lower penetration depth (3-4 mm) than small and large bowel but higher value than liver. These values are in reasonable agreement with the values of other published *in vivo* data in human normal brain, prostatic carcinoma, and esophageal carcinoma[6-9]. In our results, peritoneum shows lower penetration depth than expected value (higher than

small and large bowel) based on their histological structures. This may be due to the surface of peritoneum tends to be bloody although physicians tried to wipe off the blood as much as possible before the measurements.

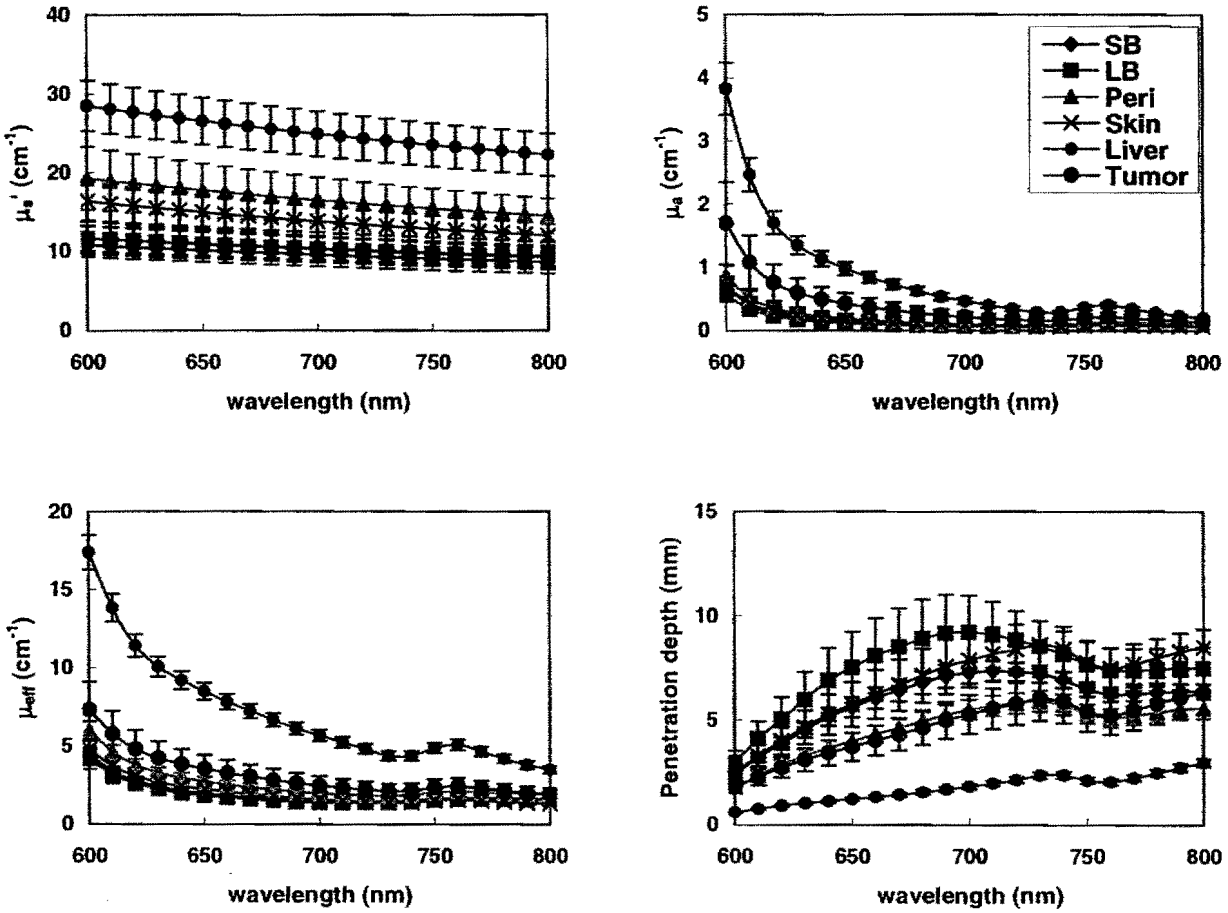

Figure 3. The average results of the extracted reduced scattering, absorption, effective attenuation coefficients, and penetration dept for small bowel (SB), large bowel (LB), peritoneum (Peri), skin, liver, and tumor before PDT.

We calculated blood oxygenation and blood volume from oxy- and deoxy-hemoglobin as described above. The results including photofrin concentration are shown in Figure 4. The values lie within the expected physiological range that normal soft tissues have oxygenation 60-80% and blood volume 50-120 μM and tumor has lower oxygenation 30-40% and higher blood volume. There is significant difference in oxygenation and blood volume before and after PDT. Tumor tends to have higher drug uptake than small bowel, large bowel, peritoneum, and skin.

Table 2. The mean values and standard deviation of the μ_s' (in cm^{-1}), μ_a (in cm^{-1}), μ_{eff} (in cm^{-1}), and penetration depth (in mm) at 630nm before and after PDT.

	Small bowel	Large bowel	Peritoneum	Tumor	Skin	Liver
μ_s' before	10.4±1.0	11.2±2.3	18.3±3.6	11.2±1.6	15.5±2.3	27.3±3.1
μ_s' after	9.3±1.3	9.2±1.5	15.2±2.2	NA	18.3±3.5	25.7±3.9
μ_a before	0.21±0.04	0.17±0.04	0.27±0.06	0.59±0.23	0.23±0.05	1.35±0.14
μ_a after	0.20±0.04	0.16±0.05	0.23±0.10	NA	0.18±0.09	1.47±0.10
μ_{eff} before	2.4±0.2	2.2±0.4	3.3±0.3	4.2±2.7	2.7±0.3	10.1±0.6
μ_{eff} after	2.2±0.2	1.9±0.4	2.7±0.5	NA	2.4±0.7	10.4±0.6
penetration depth before	4.5±0.4	6.0±1.3	3.3±0.3	3.1±0.5	4.7±0.8	1.0±0.1
penetration depth after	5.1±0.6	6.2±1.3	4.5±0.8	NA	5.9±1.0	1.0±0.1

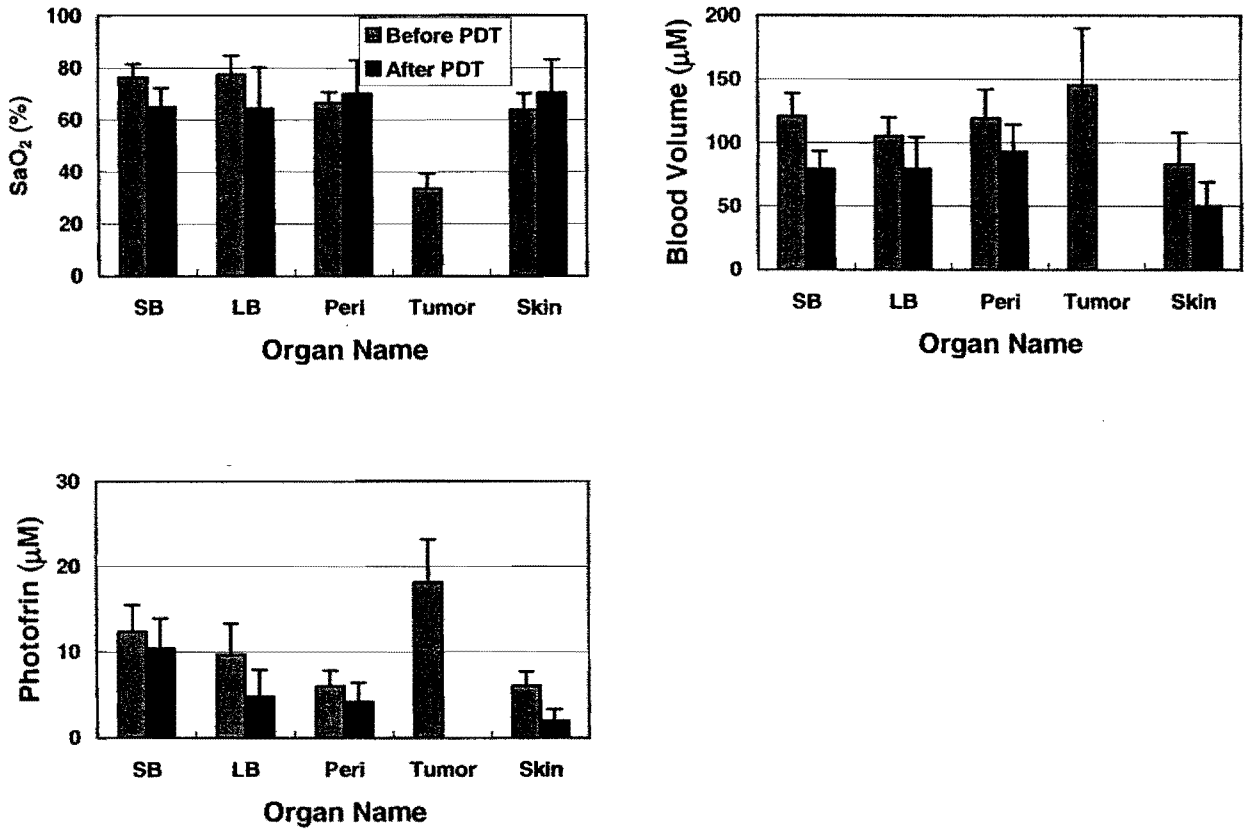

Figure 4. The blood oxygen saturation, blood volume, and Photofrin concentration in human small bowel (SB), large bowel (LB), peritoneum (Peri), tumor, and skin.

We are unable to calculate oxygenation and blood volume of liver tissues because the assumption that μ_a is composed of four major chromophores (oxy-, deoxy-hemoglobin, Photofrin, and water) may not apply. Therefore, it

introduced higher error in fitting measured reflectance spectra to calculated spectra than that in other soft tissues and generated unreasonable concentration of chromophores. However, we have investigated that the overall values in μ_s', μ_a, μ_{eff}, and penetration depth only varied slightly such that the prediction in liver optical properties is within a reasonable error range.

We have demonstrated our device and algorithm for rapid measurement and extraction of *in vivo* tissue optical properties to determine important dosimetric quantities before and after PDT. Our results Further analysis for more patients is necessary and essential to obtain a statistically satisfactory conclusion in the optical property measurement and thus the importance to PDT treatment efficacy.

REFERENCES

1. T. J. Farrell and M. S. Patterson, "A diffusion theory model of spatially resolved, steady-state diffuse reflectance for the noninvasive determination of tissue optical properties in vivo," Medical Physics 19, 879-88 (1992).
2. E. L. Hull, M.G. Nichols, and T.H. Foster, "Quantitative broadband near-infrared spectroscopy of tissue-simulating phantoms containing erythrocytes," Physics in Medicine and Biology 43, 3381-404 (1998).
3. M. Solonenko, R. Cheung, T. M. Busch, et.al., "In vivo reflectance measurement of optical properties, blood oxygenation and motexafin lutetium uptake in canine large bowels, kidneys and prostates," Physics in Medicine and Biology 47, 857-73 (2002).
4. T. Ddurduran, R. Cchoe, J. P. Culver, L. Zubkov, M. J. Holboke, J. Giammarco, B. Chance, and A. G. Yodh, "Bulk optical properties of healthy female breast tissue," Physics in Medicine and biology 47, 2847-2861 (2002).
5. S. Prahl, Optical Properties spectra (webpate http://omic.ogi.edu/spectra/index.html) (2001).
6. B. C. Wilson, P. J. Muller, and J. C. Yanch, "Instrumentation and light dosimetry for intra-operative photodynamic therapy (PDT) of malignant brain tumours," Physics in Medicine and Biology 31, 125-133 (1986).
7. P. J. Muller and B. C. Wilson, "An update on the penetration depth of 630nm light in normal and malignant human-brain tissue in vivo," Physics in Medicine and Biology 31, 1295-1297 (1986).
8. L. K. Lee, C. Whitehurst, M. L. Pantelides, and J. V. Moore, "An interstitial light assembly for photodynamic therapy in prostatic carcinoma," BJU Int 84, 821-826 (1999).
9. A. Maier, D. Sullmann, U. Anegg, F. Tomaselli, P. Rehak, H. Hutten, H. Pinter, and F. M. Smolle-Juttner, "In vivo determination of tumor optical parameters in esophageal carcinoma," Lasers Surg Med 27, 350-357 (2000).